Available online at www.sciencedirect.com
SCIENCE DIRECT®
Building and Environment 41 (2006) 254–261
BUILDING AND ENVIRONMENT
www.elsevier.com/locate/buildenv

CFD analysis of ventilation effectiveness in a public transport interchange

Zhang Lin[a,*], Feng Jiang[b], T.T. Chow[a], C.F. Tsang[a], W.Z. Lu[c]

[a]*Division of Building Science and Technology, City University of Hong Kong, Hong Kong S.A.R.*
[b]*Institute of Nuclear and New Energy Technology, Tsinghua University, Beijing*
[c]*Department of Building and Construction, City University of Hong Kong, Hong Kong S.A.R.*

Received 16 September 2004; received in revised form 21 February 2005

Abstract

A study was conducted into the ventilation effectiveness of a ventilation system within a public transport interchange (PTI) in Hong Kong. A computational fluid dynamics (CFD), steady state computational model of the PTI was used to investigate and predict the typical pollutant emission pattern for buses. In Hong Kong, the displacement ventilation (DV) scheme is often employed for the PTI. The numerical simulation investigates the effectiveness of the DV system in removing pollutants from the occupied zone. An alternative model is proposed where the supply is located at the ceiling and the exhausts are located at the lower part of the columns. It was found that both systems could adequately ventilate the PTI; however, the ceiling based air supply system is able to provide improved thermal comfort and indoor air quality (IAQ).

Keywords: Displacement ventilation; Public transport interchange; Carbon monoxide (CO); Nitrogen dioxide (NO_2); Computational fluid dynamics (CFD); Thermal comfort; Indoor air quality (IAQ); Ventilation effectiveness

1. Introduction

The recent EPA report from the US Environmental Protection Agency states that breathing diesel fumes raises a person's risk of lung cancer [1]. In addition to promoting cancer the fumes are likely to damage lungs in other ways such as causing irritation and inflammation in the lungs. Diesel engines are usually used in large trucks, buses, trains and ships. A Japanese study reported the presence of a highly carcinogenic chemical in diesel exhaust fumes. The researchers stated that this could be the highest carcinogenic chemical known to man [2]. The chemical was found to score the highest in the Ames test, which calculates the cancer-causing potential of toxic chemicals. In Hong Kong the Environmental Protection Department has implemented some measures to curb the amount of diesel fumes. The introduction of liquid petroleum gas taxis and mini-vans has been one aspect of their implementation. However, the popularity of public transport and especially large buses means that buses and heavy pollution will continue to be a feature of transportation systems in Hong Kong.

In the battle to control urban pollution, there has been several approaches to the problem. The first has been to limit the type and amount of pollutant emissions from vehicles. The second approach, which is often less emphasized, is through ventilation of buildings and public locations where there are a high number of vehicles present. The design of the ventilation system of buildings has been based on a combination of field measurements, scale model experiments and increasingly in the past few years on numerical simulation. The Hong Kong EPA initiated a field measurement study into the Lam Tin transport exchange [3]. Using field measurements results they proposed and implemented a series of

*Corresponding author. Tel.: +852 2788 9805; fax: +852 2788 9716.
E-mail address: bsjzl@cityu.edu.hk (Z. Lin).

0360-1323/$ - see front matter © 2005 Elsevier Ltd. All rights reserved.
doi:10.1016/j.buildenv.2005.02.011

improvements to improve the overall air quality. However, on-site measurements are limited by their applicability and are not relevant for other PTI. Additionally full-scale tests tend to be expensive and in some cases measurements are difficult to obtain, such as flow velocity and turbulence. The scale model approach also creates problems such as contradictory scaling factors.

The use of computational fluid dynamics (CFD) to simulate environmental and building problems has been around for over 20 years. The majority of building research investigates mainly office, residential and commercial buildings such as office and workshops. In a few cases, public areas have also been simulated such as the case of an indoor auto-racing complex by Baker [4]. CFD was used to determine the optimal way to design a ventilation system to prevent vehicle exhausts from racing cars from reaching spectators.

A series of measurements to obtain the pattern of pollution dispersion in a covered walkway was conducted by Dabberdt et al. [5]. This involved taking measurements from a wind tunnel model of a covered walkway. A similar study by Brown et al. [6] simulated a covered walkway using both a wind tunnel scale model and CFD to investigate the pollution dispersion pattern. Various ventilation schemes were adopted to determine the optimal design. It was found that the best ventilation scheme involved an overhead air supply source. Laatar et al. [7] also simulated the same problem but used a large eddy simulation (LES) turbulence model. They found that this produced better correlation with the experimental and measured data.

Several researchers have analyzed car park ventilation systems. A 3D CFD model of an underground car park was developed by Xue [8], to investigate the CO concentration. The study explores the possibility of using the CFD technique to assist in the design of the ventilation system for an underground car park. Chow et al. [9] used CFD to simulate the indoor airflow within large enclosures. This also included an indoor car park to investigate the performance of the mixed ventilation system. The simulation was validated using experimental and on site measurements and data. The indoor air quality (IAQ) of an underground building site for a car park was investigated by Fontaine et al. [10]. Several ventilation schemes were tested to find the most effective ventilation design.

The use of CFD was used by Tsou et al. [11] to simulate the pollutant pattern and dispersion of diesel fumes from public transport vehicles in a PTI. Several time transient CFD models of the proposed PTI were used to determine the best ventilation design. The studies were used to give architects and engineers more design schemes and options during the design process. There is no indication as to how the CFD data was validated in the report.

This study focuses on the implementation and design of the displacement ventilation (DV) system in the context of the PTI. Currently, the typical ventilation system used involves supply at the lower level and exhausts at the ceiling. The ability of the ventilation system to cope with the pollutants is assessed and an alternative ventilation system is proposed and investigated.

2. Computational methodology

2.1. Numerical simulation

The numerical simulation of the PTI uses the commercial CFD, CFX package to perform the analysis [12]. The program has been validated for the simulation of displacement and mixing ventilation for many types of indoor spaces such as offices, classrooms and workshops by Lin et al., [13].

Numerical simulation involves the solution to the Reynolds averaged Navier–Stokes equations and the mass conservation equation. Various types of turbulence models can be used for CFD codes, depending on the type of application. Direct numerical simulation (DNS) is considered to be the most accurate for modeling turbulent effects. LES are also used mostly for large-scale simulations. The turbulence models assume mean values of velocity rather than the actual velocity, which is difficult to simulate. Two other popular turbulence models include the k–ε model and the re-normalized (RNG) k–ε model. The *re-normalized (RNG) k–ε* model is used in this simulation. Several studies have compared the performance of these two types of models and found the latter to be more appropriate for indoor flow modeling [14]. The studies also indicate that the models are more accurate in predicting the mean velocity than the turbulent velocity.

2.2. Computational fluid dynamics (CFD) model

The governing equations for the *RNG* k–ε model are

$$\frac{\partial}{\partial t}(\rho\phi)+\frac{\partial}{\partial x_j}\left(\rho u_j\phi\right)=\frac{\partial}{\partial x_j}\left(\Gamma_\phi\frac{\partial\phi}{\partial x_j}\right)+S_\phi, \tag{1}$$

where t is the time, ρ the air density (kg/m^3), ϕ the transport variable such as enthalpy, concentration of contaminant, velocity, ϕ the u_j ($j=1$, 2, and 3) for three components of momentum, ϕ the k for kinetic energy of turbulence, ϕ the ε for dissipation rate of turbulence energy, ϕ the T for temperature, ϕ the c for contaminant concentration, x_j the coordinate, $\Gamma_{\phi,\mathrm{eff}}$ the effective diffusion coefficient, S_ϕ the source term.

Since the *RNG* k–ε model is valid for high Reynolds number turbulent flow, wall functions are needed for near wall region where the Reynolds number is

low. The present investigation uses the following wall functions:

For velocity

$$U = \left(\frac{\tau}{\rho}\right)^{1/2} \frac{1}{\kappa} \log\left(\frac{y}{y^*}E\right), \tag{2}$$

where U is the velocity parallel to the wall, τ wall shear stress, κ the von Karman constant (0.41), y the distance between the first grid node and the wall, E an integration constant (9.0), and y^* a length scale

For kinetic energy of turbulence

$$k = \frac{1}{C_\mu^{1/2}} \left(\frac{\tau}{\rho}\right). \tag{3}$$

For dissipation rate of turbulent kinetic energy

$$\varepsilon = \left(\frac{\tau}{\rho}\right)^{3/2} \frac{1}{\kappa y}. \tag{4}$$

For temperature

$$q = h_c(T_w - T). \tag{5}$$

where q is the heat flux, h_c the convective heat transfer coefficient, T_w wall temperature.

2.3. Simulation model

The model is based on the typical PTI in Hong Kong where the vehicles enter at one end and exit on the other end (Figs. 1 and 2). The buses stop at the center of the PTI, where they pick up the waiting passengers, at the passenger islands. The main supporting structures inside the PTI include seven columns evenly spaced throughout the PTI, and a wall located at the bottom of the PTI. A 3D model and plan view of the PTI showing the location of the passenger islands are shown in Figs. 1 and 2 with the basic dimensions and the PTI is closed off at the north and east walls, whereas the other two walls are open areas.

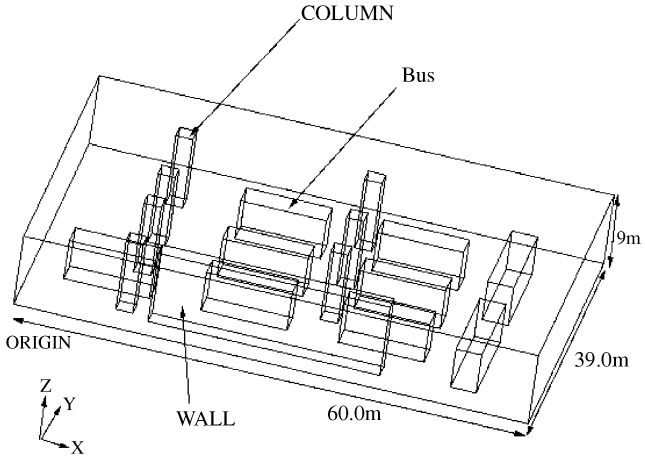

Fig. 1. A typical PTI in Hong Kong.

There are a total of nine diesel buses present in the vehicle area, each emitting NO_2 and CO. To simulate the traveling exhaust emissions, a line source is placed on the roadways. The emission rates of the vehicles are obtained from the Hong Kong environmental Protection Department Practice notes P1/98. This practice note gives typical emission rates for large buses and other vehicles. It also identifies NO_2 and CO as the main pollutants in PTI.

The simulation is initially run with the supply located at the columns and exhaust in the ceiling. This is the traditional DV design case. The simulation is then re-run with the supply in the ceiling and the exhaust at the columns. The supply is located at the ground floor level.

The entire computational domain, in the PTI is divided into a number of finite volumes by a grid system. The flow variables such as velocity, temperature and contaminant concentration are then solved at the centre of each finite volume. The size of the grid is limited by computational resources, so a mesh of $60 \times 38 \times 9$ blocks is used. The mesh is shown in Figs. 3 and 4. The Commercial code CFX uses the

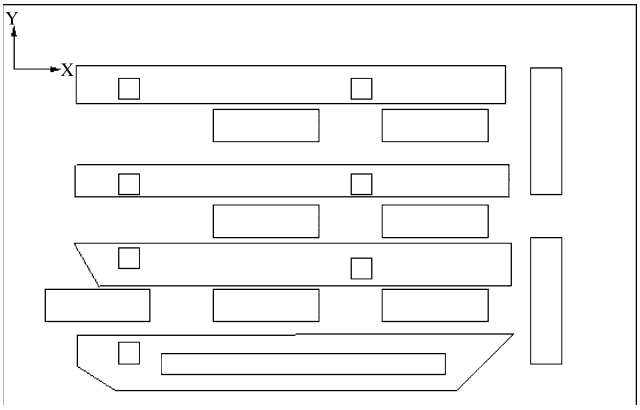

Fig. 2. Plan of PTI, with passenger island outline.

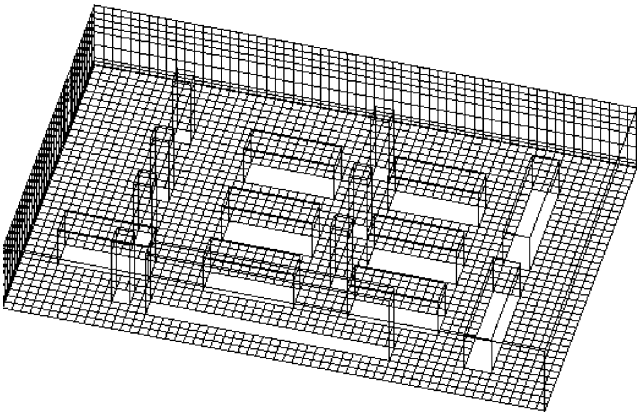

Fig. 3. 3D view of mesh.

finite-volume method and the upwind-difference scheme for the convection term.

2.4. Ventilation requirements for PTI

Typical emission rates for different vehicles were calculated by the Mass Transit Railway Corporation (MTRC) of Hong Kong in 1997. This report has been approved by the Transport Department of the Hong Kong Government. The emission factors are separated into idling and traveling cases and are shown in Table 1. Based on the traveling case, a line source can be simulated to represent the case of vehicle emissions emitted within a PTI. The figures are based on the average vehicle traveling rate of 10 km/h. The length of the traveling lane within the PTI is 60 m.

The necessary ventilation rates for CO and CO_2 dilution are calculated based on the formula suggested by the Permanent International Association of Road Congress (PIRAC) 1987, and is shown as follows:

For CO dilution

$$Q_F = q^0 \mathrm{CO}_x D_{\mathrm{pc}} 10^6 / 3600 / \mathrm{CO}_{\mathrm{lim}} \text{ (Idling).} \quad (6)$$

$$Q_{\mathrm{F}} = q^0 \mathrm{CO}_x D_{\mathrm{tc}} 10^6 / 3600 / \mathrm{CO}_{\mathrm{lim}} \text{ (Travelling).} \quad (7)$$

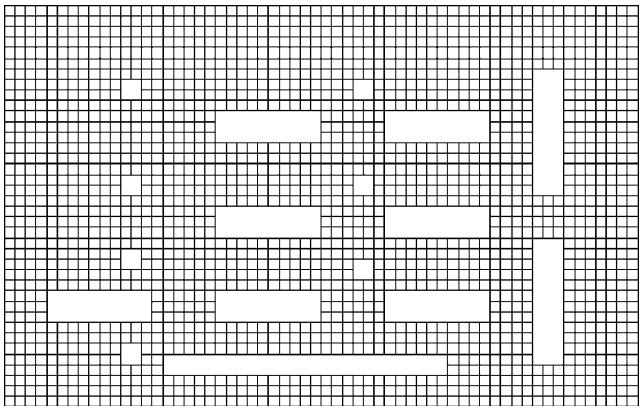

Fig. 4. Plan view of Mesh.

For NO_2 dilution

$$Q_{\mathrm{F}} = q^0 \mathrm{NO}_x D_{\mathrm{pc}} 10^6 / 3600 / \mathrm{NO}_{\mathrm{lim}} \text{ (Idling),} \quad (8)$$

$$Q_{\mathrm{F}} = q^0 \mathrm{NO}_x D_{\mathrm{tc}} 10^6 / 3600 / \mathrm{NO}_{\mathrm{lim}} \text{ (Travelling),} \quad (9)$$

Q_{f} = Required air quantity per sc $\left(\mathrm{m}^3/\mathrm{s}\right)$,

$q^0\mathrm{CO}$ = CO emission per vehicle $(\mathrm{m}^3/\mathrm{h}\,\mathrm{veh})$,

$q^0\mathrm{CO}$ = CO emission per vehicle $(\mathrm{m}^3/\mathrm{h}\,\mathrm{veh})$,

D_{pc} = number of vehicles per lane (pc/lane),

$\mathrm{CO}_{\mathrm{lim}}$ = maximum permissible CO concentration (ppm CO),

$\mathrm{NO}_{2\,\mathrm{lim}}$ = maximum permissible NO_2 concentration (ppm NO_2),

D_{tc} = number of traveling vehicles per km = M_{tc}/v,

where M_{tc} is the hourly traffic volume of traveling vehicles, V mean driving speed of vehicles.

The calculated ventilation rates are shown in Table 2. The total ventilation requirement is 633,600 m^3/h. The PTI volume is 21,600 m^3. Hence, the minimum air change per hour (ACH) is 29.33.

The air quality requirements are given by the Environmental Protection Agency of Hong Kong Pro PECC PN1/98 Control of air pollution in semi-confined PTIs [3], which recommends the maximum allowable concentration of pollutants in a semi-confined PTI, and is shown in Table 3. The 1-h average limits are the more conservative values and are used for the assessment. The above report also mentions that "NO_2 and CO are the dominant pollutants from vehicles, and these two pollutants should be used as design pollutants". Hence these two pollutants are focused in this report. The simulation also assumes that 20% of NO_X is converted to NO_2 within the PTI. The simulation assumes that there is no natural breeze within the PTI. An additional background NO_2 and CO has been accounted for in the

Table 1
Typical emission factors

Vehicle type	Emission factors			
	Idling (g/min)		Travelling (g/km)	
	NO_x	CO	NO_x	CO
Passenger car	0.2	4.0	0.83	2.16
Taxi	0.5	0.3	0.84	1.75
Minibus	0.5	0.3	1.70	1.10
Light goods vehicle	—	—	1.39	2.47
Heavy goods vehicle	—	—	5.07	7.76
Bus	2.0	2.0	9.26	8.66

Table 2
Calculation of ventilation rates

Bus			
Idling		*Travelling*	
Ventilation rate required to dilute CO level	30000.00	Ventilation rate required to dilute CO level CO_{lim} (ppm)	26.20
Maximum concentration allowed (ug/m^3)	4.00	Number of vehicles/lane in and out	109.00
Number of vehicles per lane (pc/lane)	2300.00	Driving speed (km/h)	10
Ambient concentration of CO (ug/m^3)	2.00	Emission factor (g/min-veh)	8.66
Emission factor (g/min-veh)	2.00	No of lanes	1.0
Colim (ppm)	26.20	Mtc (veh/h)	109.00
q_0CO (g/h)	120.00	Dtc (veh/km)	10.90
Q_F (m^3/s)	4.79	q_0CO (g/h)	86.60
		D (km)	0.06
		Q_F (m^3/s)	0.57
Ventilation rate required to dilute NO_2 level	300.00	Ventilation rate required to dilute CO level CO_{lim} (ppm)	0.17
Maximum concentration allowed (ug/m^3)	4.00	Number of vehicles/lane in and out	9.26
Number of vehicles per lane (pc/lane)	124.00	Driving speed (km/h)	10
Ambient concentration of NO_2 (ug/m^3)	2.00	Emission factor (g/min-veh)	1.85
Emission factor (g/min-veh)	0.2	No of lane	1
NO_2lim (ppm)	0.17	Mtc (veh/h)	109.00
q_0NO_2 (g/h)	24.00	Dtc (veh/km)	10.90
Q_F (m^3/s)	151.52	q_0CO (g/h)	18.52
		D (km)	0.06
		Q_F (m^3/s)	19.12

Table 3
Air quality guideline

Air pollutant	Maximum concentration not to be exceeded[a]	
	1-h average (μg/m^3)	5 min average (μg/m^3)
Carbon monoxide (CO)	30,000	115,000
Sulphur dioxide (SO_2)	800	1000
Nitrogen dioxide (NO_2)	300	1800

[a]Expressed at reference condition of 25 °C, 101.325 kPa.

simulation. The background reading was taken from an EPD monitoring station in Hong Kong. The background concentration was 69 μg/m^3 for NO_2 and 1270 μg/m^3 for CO.

3. Discussion of results

3.1. Velocity profile

Figs. 5 to 9 show the velocity distribution for the conventional DV design and the new ceiling supply based system. Amongst these graphs, Figs. 5 and 7 show the supply at ground level and exhaust in the ceiling for the DV system, whereas Figs. 6 and 8 are for the ceiling based supply system.

In the passenger island areas, the velocity for conventional system at the occupant breathing level is

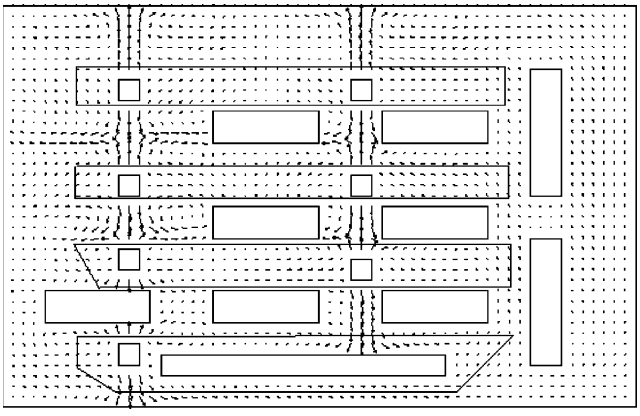

Fig. 5. Velocity profile, showing supply at $h = 1.1$ m.

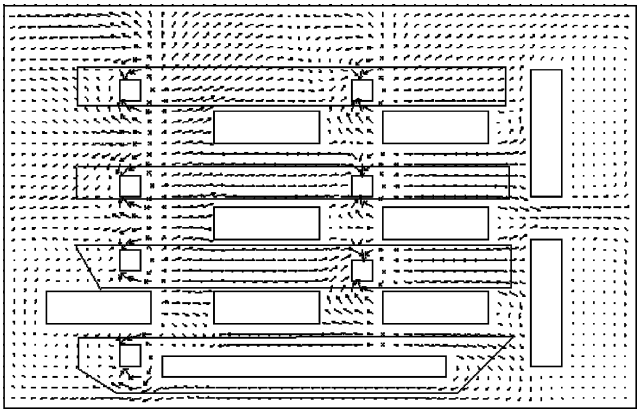

Fig. 6. Velocity profile, showing exhaust at $h = 1.1$ m.

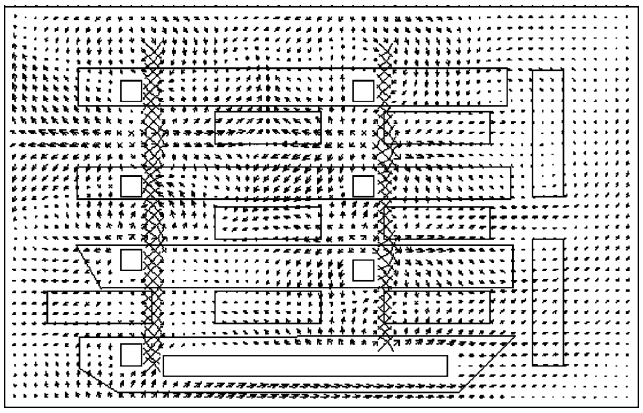

Fig. 7. Velocity profile, showing exhaust at $h = 9.0$ m.

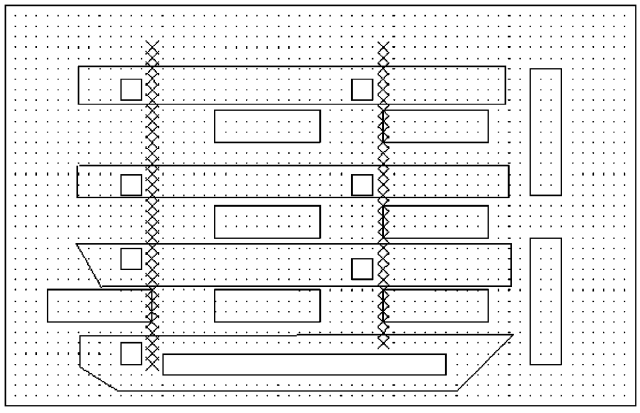

Fig. 8. Velocity profile, showing supply at $h = 9.0$ m.

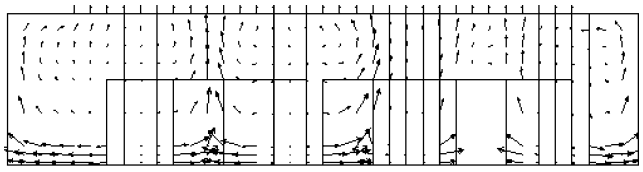

Fig. 9. Sectional velocity profile for conventional column supply.

high (typically, less than 2 m/s). In the ceiling based supply system the velocity at the occupant breathing level is lower at less than 0.5 m/s. This suggests possibly lower levels of draft effect of the new system, showing improved thermal comfort levels. However, in practice, the constant movement of vehicles suggests that occupants will inevitably experience thermal discomfort due to air disturbance. In the new system, the air falls down unimpeded directly to the occupants providing fresh air in the breathing zone. A layer of fresh air is produced at the location beneath the supply inlets, as shown in Fig. 10.

3.2. NO_2 contaminant distribution

The level of NO_2 is given in $\mu g/m^3$ and is shown for a typical breathing height of 1.6 m in Figs. 11 and 12. The conventional displacement system has a tendency to spread and displace the pollutants into the occupant-breathing zone. The ceiling supply inlets are located at $x = 13.5$ and 5.5. Examining these sections, we find that the pollutant levels are between 60 and 100 $\mu g/m^3$, for the conventional system. In the new ceiling supply system, we find substantially lower NO_2 levels ($< 20\ \mu g/m^3$). This is illustrated in Figs. 13–16. In the conventional system, the NO_2 levels gradually decrease from 100 to 40 $\mu g/m^3$. The highest levels being in the occupant-breathing zone, while lower values in the area of the ceiling.

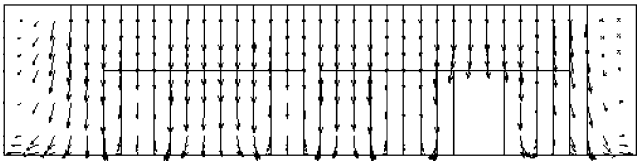

Fig. 10. Sectional velocity profile for proposed ceiling supply.

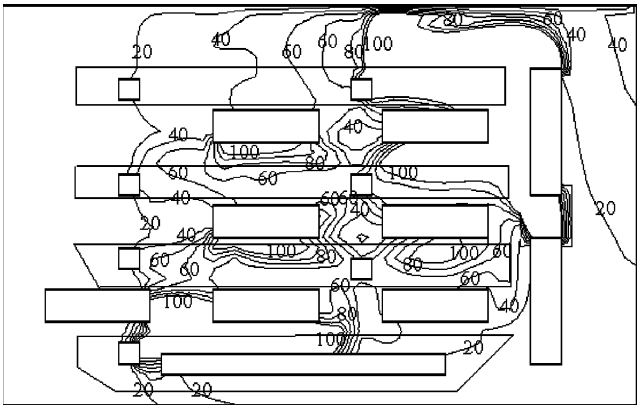

Fig. 11. NO_2 distribution at $h = 1.6$ m ($\mu g/m^3$) for convention system.

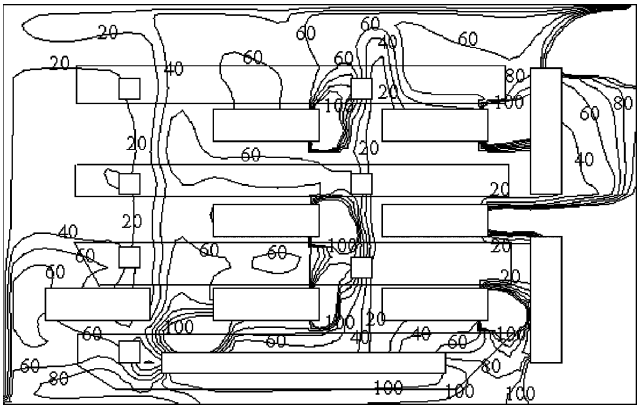

Fig. 12. NO_2 distribution at $h = 1.6$ m ($\mu g/m^3$) for proposed system.

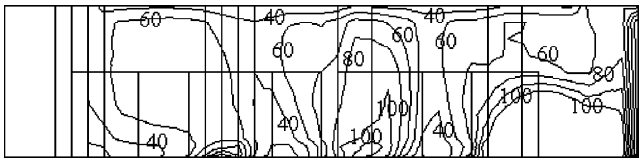

Fig. 13. NO_2 distribution at $x = 13.5$ m ($\mu g/m^3$) for convention system.

Fig. 14. NO_2 distribution at $x = 13.5$ m ($\mu g/m^3$) for proposed system.

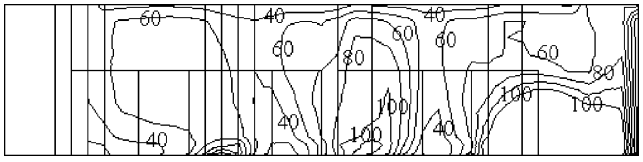

Fig. 15. NO_2 distribution at $x = 35.5$ ($\mu g/m^3$) for convention system.

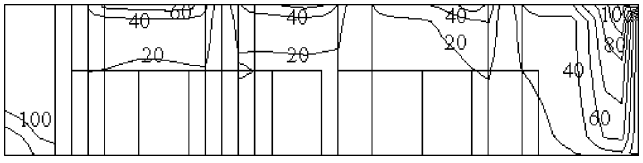

Fig. 16. NO_2 distribution at $x = 35.5$ m ($\mu g/m^3$) for proposed system.

The location of the supply in the ceiling effectively results in a stratum of fresh air which clears the NO_2 from the area directly beneath. The fresh air zone created by the supply also suggests the possibility that a wall of air could be used to separate occupants from vehicle pollutants. Examining the airflow for the conventional where the supply comes from the columns the result is to disperse the NO_2 throughout the PTI and, in particular, exacerbate the pollution levels at the breathing zone.

In terms of the passenger island areas, we can see that where there is a ceiling supply above that section of the passenger zone then the NO_2 levels are very low (typically <20 ($\mu g/m^3$). This shows that the most effective method of clearing pollutants is through placing the supply inlets in the ceiling directly above the passenger islands. It should be noted that the effectiveness is not based on the exhaust removing the contaminants but on the supply of fresh air from the ceiling creating a layer of fresh air. It was also found that the levels are within 300 $\mu g/m^3$ as stipulated in Table 3. Higher NO_2 levels are present at the northeast of the PTI, suggesting inadequate ventilation at this particular area.

3.3. CO contaminant distribution

The CO levels are shown in Figs. 9–11. A similar pattern to the NO_2 is observed. Again examination of the ceiling based supply system shows that it is more effective than the column based supply system. The values of CO for the ceiling based supply system are around 100 $\mu g/m^3$ (Fig. 10b and Fig. 11b) in comparison to 200–500 $\mu g/m^3$ for the DV system. The highest values of carbon dioxide are at the location of the engine exhaust, where values are >500 $\mu g/m^3$. However, it should be noted that the CO levels are all within the levels limited by Table 3 of 30,000 $\mu g/m^3$. The CO levels are slightly higher than the NO_2 levels (Figs. 17–22), but the CO levels allowed are significantly higher than the NO_2 levels.

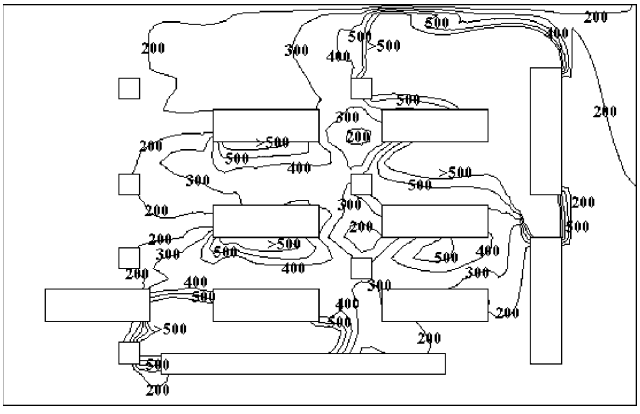

Fig. 17. CO distribution at $h = 1.6$ m ($\mu g/m^3$) for convention system.

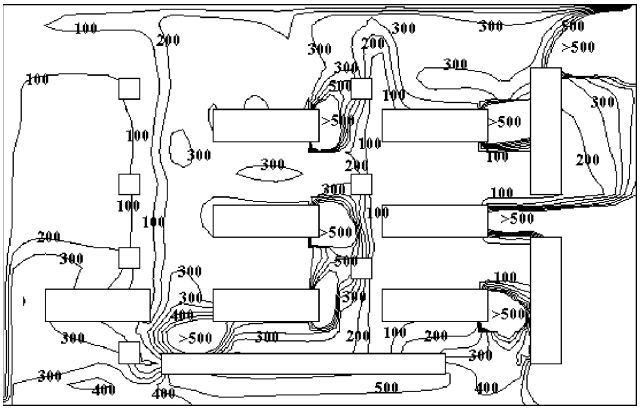

Fig. 18. CO distribution at $h = 1.6$ m ($\mu g/m^3$) for proposed system.

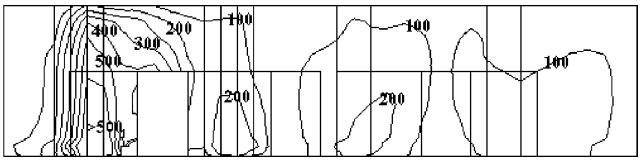

Fig. 19. CO distribution at $x = 13.5$ m ($\mu g/m^3$) for convention system.

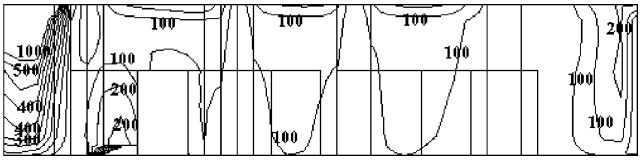

Fig. 20. CO distribution at $x = 13.5$ m ($\mu g/m^3$) for proposed system.

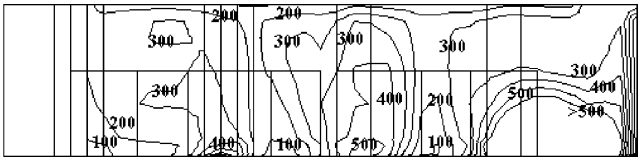

Fig. 21. CO distribution at $x = 35.5$ ($\mu g/m^3$) for convention system.

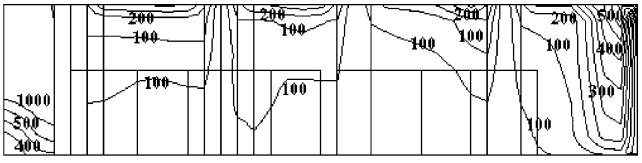

Fig. 22. CO distribution at $x = 35.5$ m ($\mu g/m^3$) for proposed system.

4. Conclusion

The results indicate that the use of the conventional (DV) system to disperse pollutants in a PTI is not effective. The ventilation system blows the pollutants directly into the occupant-breathing zone resulting in a bad air quality in the occupied zone. The close proximity of the supply to occupants shows high draft effects and bad thermal comfort. The better result is obtained for the case where the supply is in the ceiling and the exhaust is close to the ground. A ceiling based ventilation supply system significantly improves the IAQ of a PTI. However, both systems were able to provide adequate IAQ for the PTI since the values of CO and NO_2 were within the limits given by Table 3.

Acknowledgement

The work was supported by Strategic Research Grant no. 7001589 of the City University of Hong Kong.

References

[1] Health assessment document for diesel engine exhaust. USEPA EPA/600/8-90/057F, 01 May 2002. US Environmental Protection Agency, Office of Research and Development, National Centre for Environmental Assessment, Washington, DC.
[2] Enya T, Suzuki H, Watanabe T, Hirayama T, Hisamatsu Y. 3-Nitrobenzanthrone, a powerful bacterial mutagen and suspected human carcinogen found in diesel exhaust and airbourne particulates. Environmental Science and Technology 1997;31: 2772–6.
[3] Environmental Protection Department, Hong Kong: air quality improvement for Lam Tin transport interchange. Report no. EPD/TP9/96.
[4] Baker AJ. Design of a ventilation system for an indoor auto racing complex. 2002 ASHRAE winter meeting, January 13–16, 2002.
[5] Dabbert WF, Huydysh WG, Read M. Pollution dispersion at complex street configurations: covered roadways. Presented at the fourth international symposium on transport and air pollution, June 9–13, Avignon, France, 1997.
[6] Brown AL, Dabbert WF. Modeling ventilation and dispersion for covered walkways. Journal of Wind Engineering and Industrial Aerodynamics 2003;91(5):593–608.
[7] Laatar AH, Benahmed M, Belghith A, Le Quere P. 2D large eddy simulation of pollutant dispersion around a covered walkway. Journal of Wind and Engineering Industrial Aerodynamics 2002;90(6):617–37.
[8] Xue H, Ho JC. Modelling of heat and carbon monoxide emitted from moving cars in an underground car park. Tunnelling and Underground Space Technology 2000;15(1):101–15.
[9] Chow WK. Ventilation design: use of computational fluid dynamics as a study tool. Building Service Engineering Research and Technology 1995;16(2):63–76.
[10] Fontaine JR, Rapp R. The design of ventilation systems of large enclosures with unconfined pollutant sources. Fifth international conference on air distribution in rooms. Room Vent '96, vol. 3. July 19. p. 95–102.
[11] Tsou JY, Zhu Yimin, Lam S. Improving air quality of public transport interchanges design. Strategies to integrate CFD simulation in early design process. Architectural information management −02 design process vol. 1. p. 54–9.
[12] AEA technology, CFX-4.2 environment user manual, vol. 1–4. 1997.
[13] Lin Z, Chow TT, Fong KF, Wang Q. Validation of CFD model for research into the application of displacement ventilation to Hong Kong Buildings. The proceedings of the third international symposium on HVAC, Shenzhen, China, vol. 2. p. 602–13.
[14] Chen Q. Comparison of different $k-\varepsilon$ models for indoor air flow computations. Numerical Heat Transfer 1995;28(Part B): 353–69.